

**Project Report**  
**LSP-255**

**Small-Sat-Ladar Final Report:  
FY18 Integrated Systems  
Line-Supported Program**

C.A. Primmerman

4 February 2019

---

**Lincoln Laboratory**  
MASSACHUSETTS INSTITUTE OF TECHNOLOGY  
*LEXINGTON, MASSACHUSETTS*



---

This material is based upon work supported by the Under Secretary of Defense for Research and  
Engineering under Air Force Contract No. FA8702-15-D-0001.

DISTRIBUTION STATEMENT A. Approved for public release. Distribution is unlimited.

This report is the result of studies performed at Lincoln Laboratory, a federally funded research and development center operated by Massachusetts Institute of Technology. This material is based upon work supported by the Under Secretary of Defense for Research and Engineering under Air Force Contract No. FA8702-15-D-0001. Any opinions, findings, conclusions or recommendations expressed in this material are those of the author and do not necessarily reflect the views of the Under Secretary of Defense for Research and Engineering.

© 2019 Massachusetts Institute of Technology

Delivered to the U.S. Government with Unlimited Rights, as defined in DFARS Part 252.227-7013 or 7014 (Feb 2014). Notwithstanding any copyright notice, U.S. Government rights in this work are defined by DFARS 252.227-7013 or DFARS 252.227-7014 as detailed above. Use of this work other than as specifically authorized by the U.S. Government may violate any copyrights that exist in this work.

**Massachusetts Institute of Technology  
Lincoln Laboratory**

**Small-Sat-Ladar Final Report: FY18 Integrated  
Systems Line-Supported Program**

*C.A. Primmerman  
Division 9*

**Project Report LSP-255**

**4 February 2019**

**DISTRIBUTION STATEMENT A. Approved for public release. Distribution is unlimited.**

**Lexington**

**Massachusetts**

**This page intentionally left blank.**

## TABLE OF CONTENTS

	Page
List of Illustrations	v
1. INTRODUCTION AND OVERVIEW	1
2. SMALL-SAT-LADAR TRADE SPACE	3
3. ADVANTAGES OF FLYING LOW	5
4. ELEMENTS OF SMALL-SAT LADAR	7
5. GENERAL CONCEPT OF OPERATION	9
6. ELECTRIC PROPULSION	11
7. FIBER-LASER TRANSMITTER	13
8. PHOTON-COUNTING RECEIVER	15
9. DATA-DRIVEN REGISTRATION	17
10. PACKAGING	19
11. CONCLUSIONS	23
References	25

**This page intentionally left blank.**

## LIST OF ILLUSTRATIONS

Figure No.		Page
1	Small-sat-ladar 3D ground-imaging system.	2
2	The trade space considered for the small-sat ladar.	3
3	Total satellite mass versus aperture size for various commercial earth-imaging satellites.	5
4	Satellite mass versus orbital altitude.	6
5	The major elements of the small-sat ladar.	7
6	The small-sat ladar has two modes of operation: a 3D-mapping mode for open terrain and a foliage-penetration (FoPen) mode.	9
7	Optical payload schematic.	10
8	Drag force versus orbit altitude for a 0.5 m <sup>2</sup> cross section.	11
9	Thrusters for the small-sat ladar.	12
10	Requirements for the small-sat-ladar transmitter.	13
11	Four different focal-plane options for the small-sat ladar.	15
12	Modular Geiger-mode APD cameras.	16
13	Data-driven jitter compensation.	17
14	Simulation of the data-driven jitter compensation.	18
15	Small-sat-ladar packaging.	19
16	Front and back isometric views of the small-sat-ladar system.	20
17	Estimates of the mass and power allocations.	21

**This page intentionally left blank.**



# 1. INTRODUCTION AND OVERVIEW

Airborne 3D imaging ladars such as ALIRT<sup>i</sup> and MACHETE<sup>ii,iii</sup> have demonstrated operational utility in Afghanistan and in the SOUTHCOM area of responsibility. They have been used for mapping (Afghanistan is, perhaps, the best mapped country in the world.), detecting objects under foliage and camouflage, route planning, change detection, determining vehicle accessibility, identifying helicopter landing zones, and supporting planning for special-forces operations. Extending 3D imaging to space would provide similar capabilities for denied territory. A problem with space systems, of course, is that they can be very large and costly. The objective of the study described in this report was to develop a small-sat-ladar concept that has good performance but reasonably low cost.

This study was funded by the Integrated Systems portion of the MIT Lincoln Laboratory (MIT LL) Line.<sup>iv</sup> It was conducted from FY17 through FY18.

The concept developed has the following general characteristics:

- it uses efficient fiber lasers and photon-counting detectors to achieve high performance in a low-weight system;
- it fits in an ESPA-class satellite;
- it flies in a very low orbit (~220 km) to get ~50-cm cross-range resolution at nadir; and
- it is able to generate image areas of about 10 km<sup>2</sup>, as shown in Figure 1.

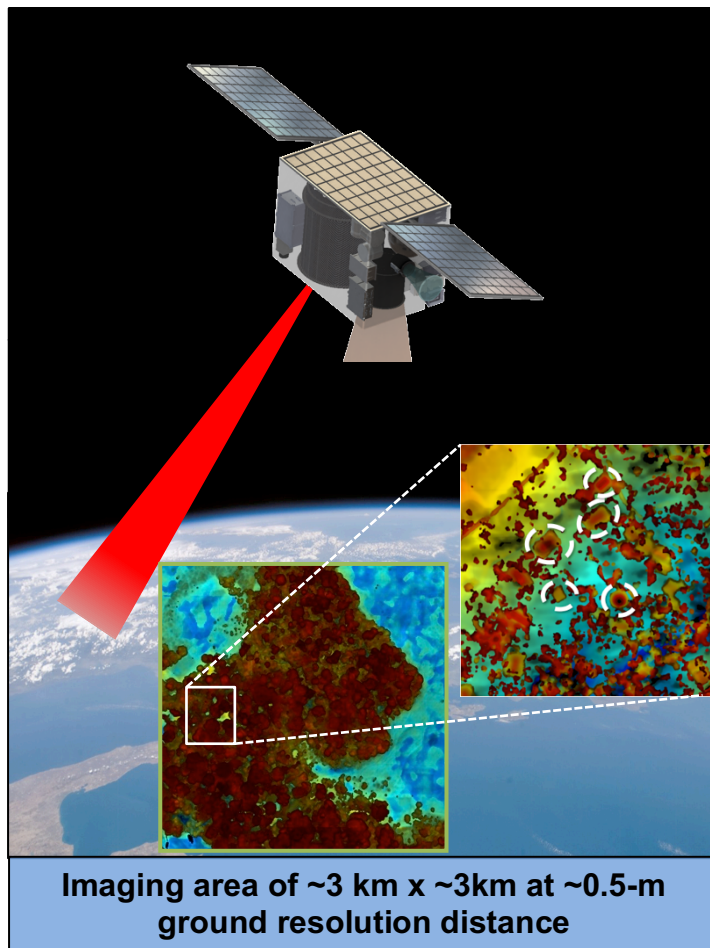


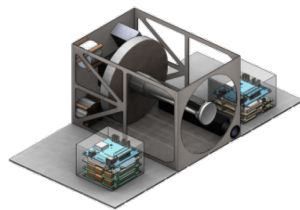
*Figure 1. Small-sat-ladar 3D ground-imaging system.*

## 2. SMALL-SAT-LADAR TRADE SPACE

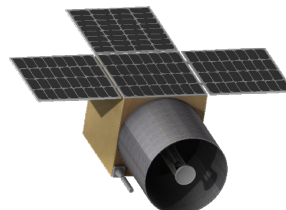
Figure 2 shows the trade space considered for the small-sat ladar. First, a cubesat ladar flying at 400-500 km was examined. This concept is attractive for its small size and cost, but the ground resolution of ~3 m was deemed unacceptable. Next, we considered a 50-cm aperture flying at 400-500 km. This system would have a ground resolution of ~1 m, which still is rather coarse for many applications of interest. Finally, we considered a 50-cm aperture flying in very low-earth orbit at about 220 km. As will be discussed later, this altitude has the disadvantage that it requires continuous propulsion to maintain its orbit, but it has the advantage that it achieves a cross-range resolution of ~50 cm. The remainder of this report will focus on this low-flying system.



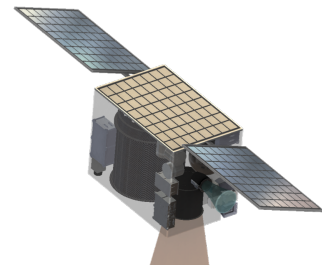
### Small-Sat-Ladar Trade Space



Cubesat with 20cm aperture and deployable electronics



ESPA-class satellite with 50cm aperture and no propulsion



ESPA-class satellite with 50cm aperture and electric propulsion

	Cube Sat (LEO)	Small Sat (LEO)	Small Sat (NEO)
<b>Altitude</b>	400-500 km	400-500 km	220 km
<b>Propulsion</b>	No	No	Yes
<b>Bus</b>	16U	ESPA-Size	ESPA-Size
<b>Aperture</b>	20-cm	50-cm	50-cm
<b>GRD</b>	2.6-3.2 m	1.0-1.3 m	0.57 m

Ground Resolution Distance (GRD) =  $1.22\lambda R/D = 1.22(1.06\mu\text{m})R/D$

CAP-9  
25 July 2018

LINCOLN LABORATORY  
MASSACHUSETTS INSTITUTE OF TECHNOLOGY

Figure 2. The trade space considered for the small-sat ladar.

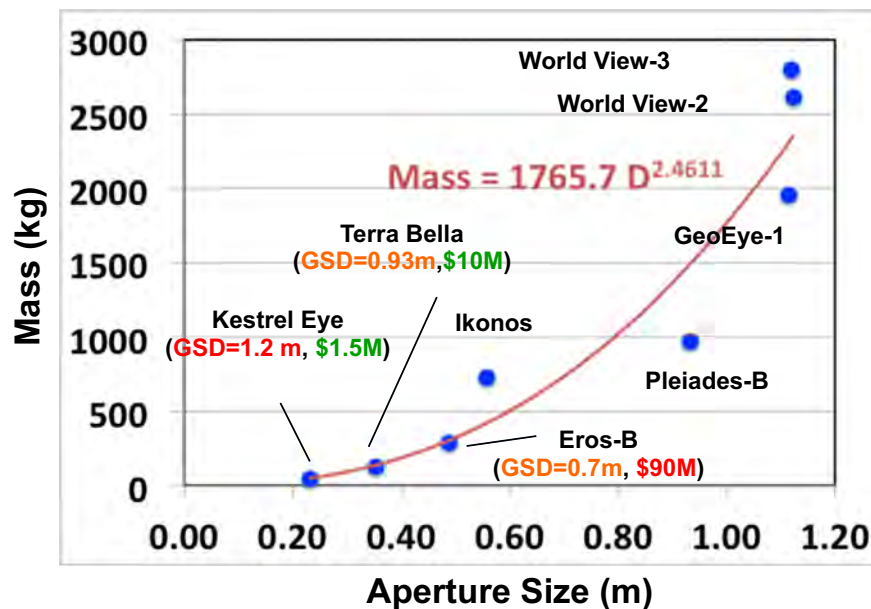
**This page intentionally left blank.**

### 3. ADVANTAGES OF FLYING LOW

Figure 3 shows a plot of total satellite mass versus aperture size for various commercial earth-imaging satellites. We see that the mass goes as approximately  $D^{2.5}$ . Thus, aperture size is a significant driver for the mass of a space-based optical-imaging system. Since satellite cost tends to go as the weight of the satellite, aperture size is also a significant driver for overall cost.



## Aperture-Mass Scaling for Commercial High-Resolution Earth Imagers



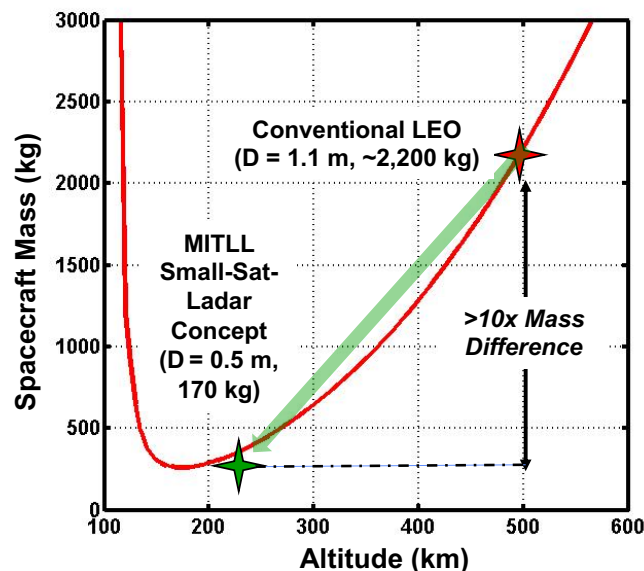
Aperture size is significant mass (and cost) driver for EO ISR systems

Figure 3. Total satellite mass versus aperture size for various commercial earth-imaging satellites.

The satellites in Figure 3 are at different altitudes and have different ground resolutions. If we specify the ground resolution and want to minimize the satellite mass (and cost), we can generate a curve, such as shown in Figure 4, giving satellite mass versus orbital altitude. For this curve we have specified the ground resolution to be 50 cm and have taken a wavelength of  $1.06\ \mu\text{m}$  (a wavelength at which high-efficiency lasers are available). We see that at higher altitudes the mass goes as the altitude to the 2.5 power because the aperture diameter scales as the altitude to keep the resolution fixed. At very low altitudes, the mass increases dramatically because of the propulsion required to maintain the orbit. We find that there is a minimum mass at an orbit altitude of about 200 km. As we will see later, our small-sat-ladar concept flying at 220 km has a mass of 170 kg. This mass is less than a tenth of the mass of a similar-performance system flying at a more conventional altitude of 500 km.



## Design Space for 50-cm GRD (at $1.06\ \mu\text{m}$ ) Space-Based Ladar System



**Lower altitude improves performance and lowers system cost significantly**

Figure 4. Satellite mass versus orbital altitude.

## 4. ELEMENTS OF SMALL-SAT LADAR

Major elements of the small-sat ladar are shown in Figure 5. The ladar is implemented on an ESPA sized custom bus configured to minimize drag. It is estimated to have a wet weight of 170 kg and to require an orbit-averaged power of 230 W. To keep the satellite at its altitude of 220 km for up to five years there is continuous thrust from electric propulsion systems.

A compact 50-cm telescope is packaged in the ESPA-sized satellite. The transmitter laser is a high-efficiency 200-W fiber laser operating at 1.06  $\mu\text{m}$ ; the laser produces  $< 5\text{-ns}$  pulses at a repetition rate of  $> 200\text{ kHz}$ . Return pulses are detected by a 256 x 256 Geiger-mode APD array. To reduce the need for heavy inertial pointing systems, registration of the ladar data is accomplished using a novel image-based registration algorithm.

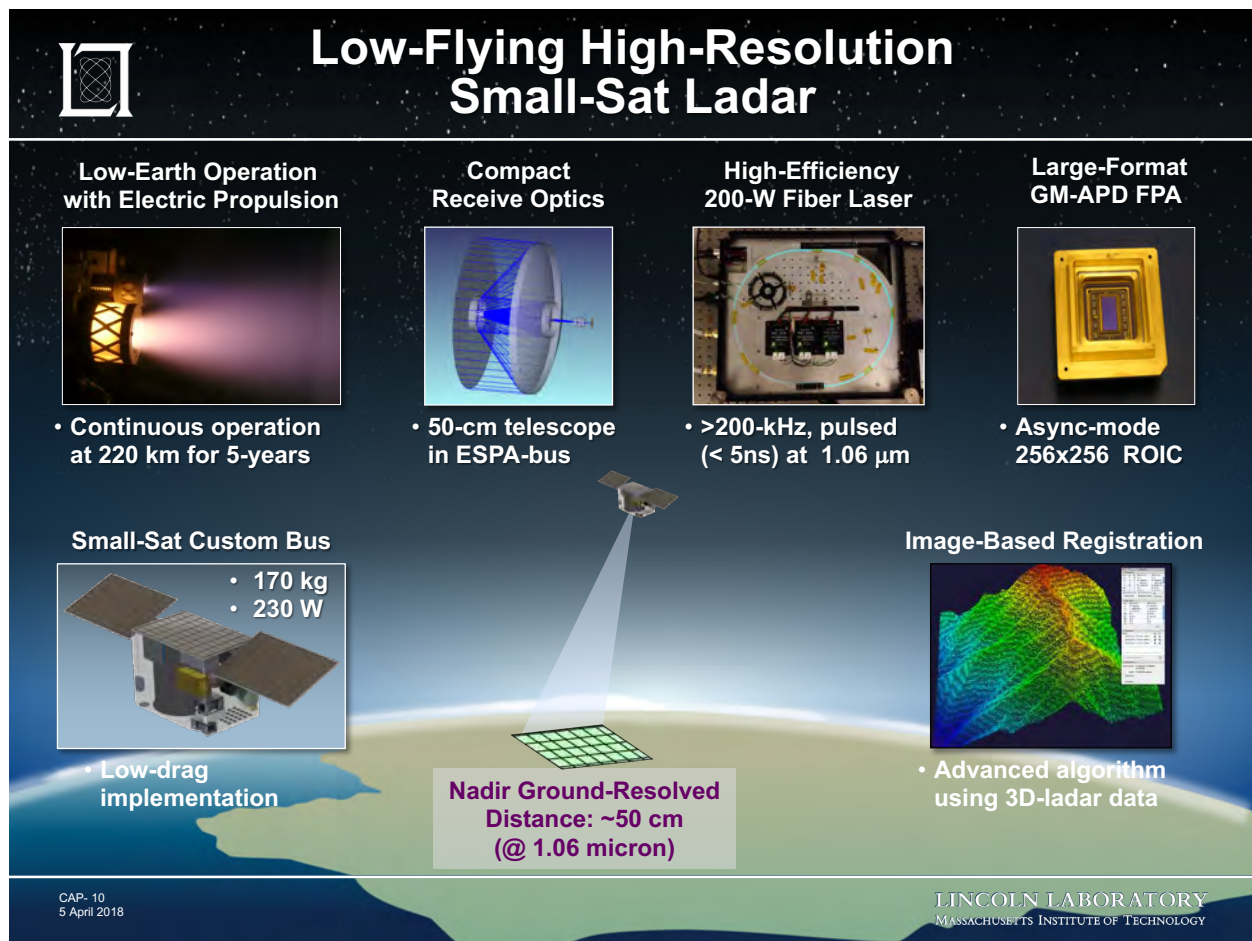


Figure 5. The major elements of the small-sat ladar.

**This page intentionally left blank.**



## 5. GENERAL CONCEPT OF OPERATION

Figure 6 shows two modes of operation for the small-sat lidar: a 3D-mapping mode for open terrain and a foliage-penetration (FoPen) mode. In both modes the lidar images an area on the ground for  $\sim 35$  s, while it is between nadir angles of  $-35^\circ$  and  $+35^\circ$ . Instantaneously, the laser illuminates an approximately 70-m x 70-m area on the ground (corresponding to about 128 x 128 APD pixels).

For the 3D-mapping mode, the satellite is body pointed to the center of the area being imaged, and a fast-steering mirror (FSM) scans the laser across a roughly 3.5-km x 3.5-km area to build up the image. For the FoPen mode, assuming a 90% obscuration, the area that can be imaged is about 1 km x 1 km (i.e., the area is 10% of what can be imaged in open terrain). Scanning is done at exactly the same rate, so that the 1-km x 1-km area is scanned in about three seconds. The lidar does 10-12 3-s scans, which gives the angular diversity necessary for good foliage penetration.

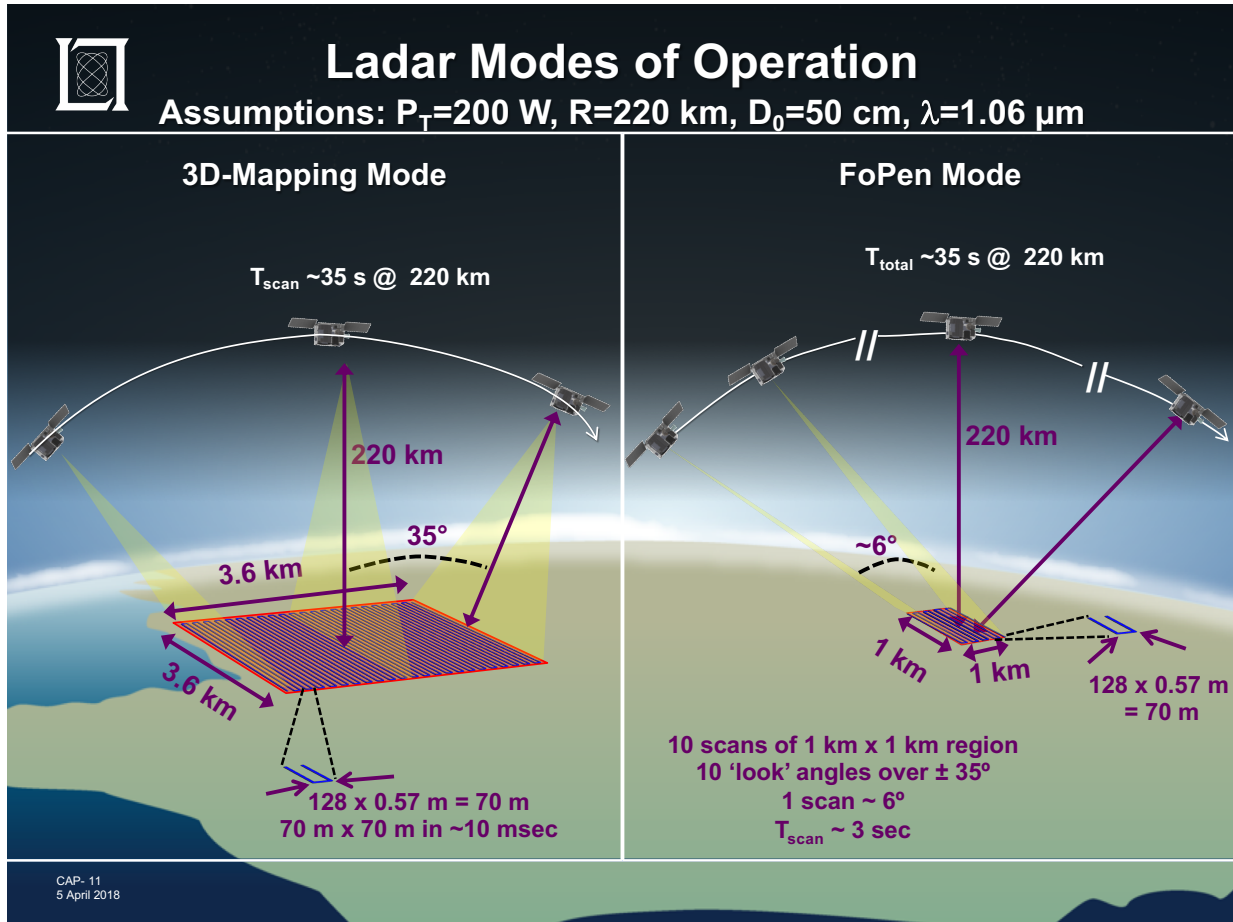


Figure 6. The small-sat lidar has two modes of operation: a 3D-mapping mode for open terrain and a foliage-penetration (FoPen) mode.

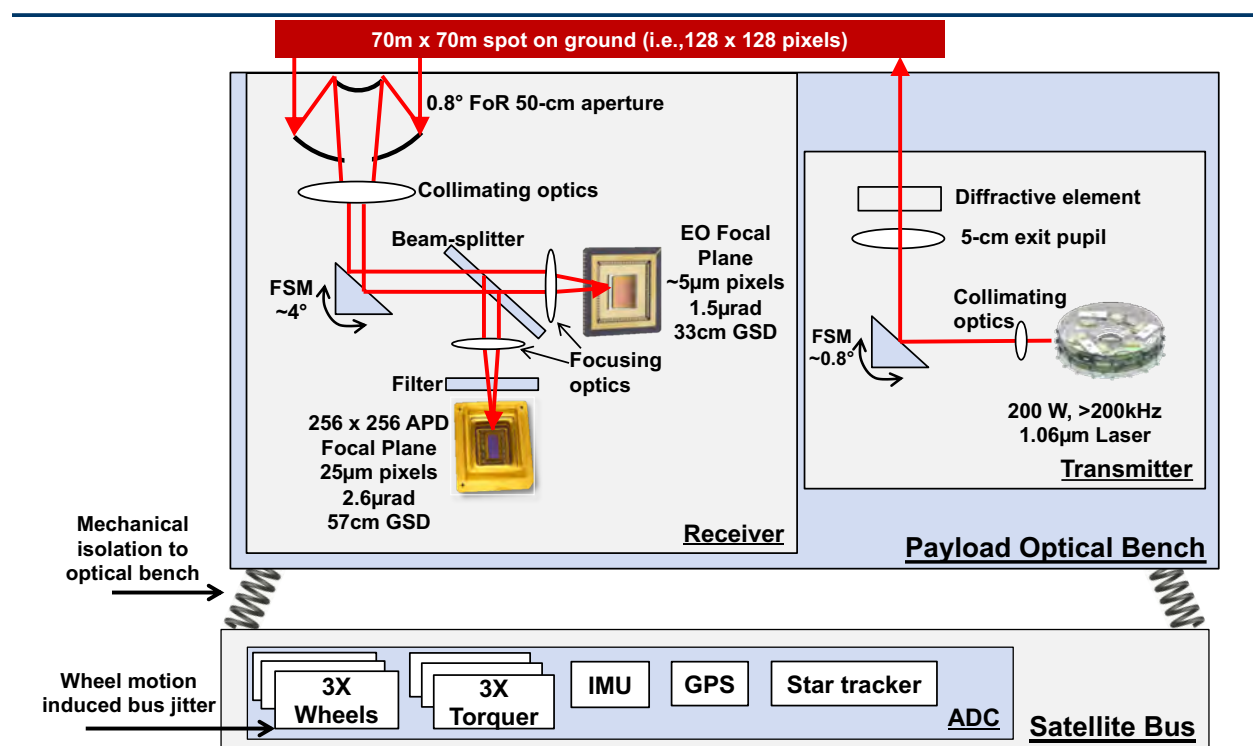
Figure 7 gives a general schematic of the optics. The laser is transmitted through its own separate aperture to minimize backscatter into the receiver. Since the laser illuminates a 70-m x 70-m spot on the ground, it can be transmitted out of a relatively small aperture ( $\sim 5$ -cm). A FSM steers the beam over a total angle of  $\sim 0.8^\circ$ . A diffractive element is incorporated to make the illuminated spot on the ground roughly square.

The backscattered light is received by a 50-cm telescope with a  $0.8^\circ$  field of regard (FoR). The receiver has its own FSM, which scans in concert with the transmitter FSM to keep the backscattered light centered on the APD focal plane. The APD array has  $25\mu\text{m}$  pixel, each corresponding to approximately  $2.6\mu\text{rad}$  in output space. There is also a contextual passive visible camera. This passive camera has its own imaging optics because the F/number for the visible camera is much smaller than that for the APD camera.

The optical system is described in much more detail in another document.<sup>v</sup>



## Optical Payload Schematic



CAP-12  
25 July 2018

LINCOLN LABORATORY  
MASSACHUSETTS INSTITUTE OF TECHNOLOGY

Figure 7. Optical payload schematic.

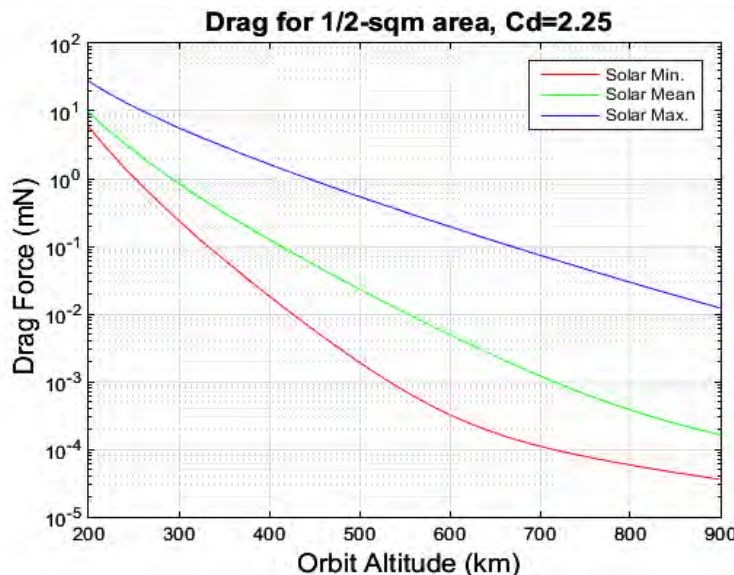
## 6. ELECTRIC PROPULSION

Electric propulsion is necessary to offset the drag for the small-sat ladar operating at 220 km. Our ESPA-sized satellite has a cross section of  $0.4 \text{ m}^2$ . For some margin, we assume a  $0.5 \text{ m}^2$  cross section. The drag force versus orbit altitude for a  $0.5 \text{ m}^2$  cross section is shown in Figure 8. We observe two things from this figure: 1) the drag at 220 km is about two orders of magnitude larger than that at a more conventional low-earth orbit of 500 km, and 2) the drag varies considerably depending on the solar cycle. The drag force for our satellite at 220 km varies from 4 - 20 mN. The design calls for two 13-mN thrusters.

We note that the European Space Agency (ESA) Gravity Field and Stead-State Ocean Circulation Explorer (GOCE) satellite provides an existence proof for the ability to fly in very low-earth orbit for extended lifetimes. GOCE lasted for 4 years, 8 months at altitudes between 235 km and 250 km. It had an approximately  $1\text{-m}^2$  cross section, giving it approximately 10-mN drag. To compensate this drag it used two 20-mN thrusters.



### Electric Propulsion to Offset Drag for Small-Sat Ladar at 220 km



#### Small-sat-ladar concept:

- Has  $0.4 \text{ m}^2$  cross-section
- For margin, assume  $0.5 \text{ m}^2$
- Drag at 220 km is 4-20 mN, depending on solar cycle
- Plan to have 2 13-mN thrusters

#### GOCE 2009 ESA mission:

- Lasted 4 years, 8 months between 250 km and 200 km
- $\sim 1\text{-m}^2$  cross-section, 10-mN drag
- Used 2 20-mN thrusters

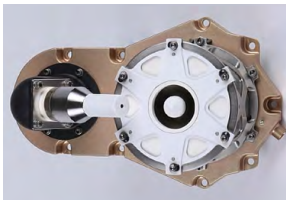
Figure 8. Drag force versus orbit altitude for a  $0.5 \text{ m}^2$  cross section.

As shown in Figure 9, the thrusters chosen for the small-sat ladar are Busek BHT-200 Hall-effect thrusters. These thrusters have been demonstrated in previous spacecraft. Further developments in thrusters—for instance, using iodine instead of xenon as the propellant—are expected to result in higher efficiency, allowing for either smaller systems or longer lifetime for the same size system.



## Thrusters for Small-Sat Ladar

- Hall-effect ion thrusters selected for low-thrust, continuous operation
  - High Isp provides a low-mass solution
- Busek BHT-200 has a high TRL (flown on Tac-Sat 2 and FalconSat-5)
- Features low heat dissipation to spacecraft, variable thrust
- Future development includes design optimization for low-SWaP and long life, alternative fuel (iodine versus xenon)



An 80 hour validation test was performed to benchmark the new iodine feed system for the BHT-200 small-satellite Hall thruster

Table 1 BHT-200-I thrust levels at the beginning and end of the 80-hr duration test.

	0-hr		80-hr	
	Xenon	Iodine	Xenon	Iodine
Discharge Voltage, V	250	250	250	250
Discharge Current, A	0.81	0.83	0.80	0.84
Thrust, mN	12.9	14.2	13.2	13.9

Figure 9. Thrusters for the small-sat ladar.

## 7. FIBER-LASER TRANSMITTER

Requirements for the small-sat-ladar transmitter are shown in Figure 10. These requirements can best be achieved using a fiber laser. The high-efficiency of fiber lasers leads to high average power with low SWaP. The 200-W laser is expected to weigh only about 6 kg. Although fiber lasers do not have space heritage, they benefit from strong recent developments, both in industry and at MIT LL. Beam-combined fiber lasers provide power scaling, if powers beyond 200 W are needed. Packaging advantages include misalignment-free design and distributed thermal load. A minor disadvantage is that peak-power limitations in the fiber mean that the ladar will need to operate at high repetition rate ( $> 100$  kHz).

Two options have been explored for the laser: a highly doped fiber and a trench fiber. Characteristics of these two fiber lasers are shown in the figure below. Both fiber lasers have been performance tested in the laboratory. In addition, certain space qualification tests have been performed, including radiation testing and lifetime testing. It appears that either fiber-laser system could meet the requirements of the small-sat ladar. Fiber-laser development and testing is described in much more detail in another document.<sup>vi</sup>



### Options for High-Power Pulsed Fiber Amplifiers

Small-Sat-Ladar Requirements		High-Energy Laser	Photonic Crystal Fiber (PCF)	Highly Doped Fiber (HDF)	Trench Fiber (TF)
Parameter	Value				
Wavelength	1030 nm or 1060 nm				
Pulse duration	<5 ns				
Pulse repetition rate	<1 MHz				
Average power	200 W				
Beam quality	<1.15 M <sup>2</sup>				
Spectral bandwidth	<1 nm				
Run time	> 40 s				
Duty cycle	> 2%				
Lifetime	5 years on orbit				
Battery cycles	90,000				
Fiber length		10.8 m	1.5 m	0.15 m	1.3m
Beam diameter		20 $\mu$ m	30 $\mu$ m	36 $\mu$ m	25 $\mu$ m $\rightarrow$ 40 $\mu$ m
>100kW pulsed operation		No	Yes	Yes	Yes
Demo performance			200W, 1mJ 5ns, 200kHz	100W, 1mJ 5ns, 100kHz	200W, 1mJ, 5ns, 200kHz
Beam quality		Near diffraction-limited			
Coil diameter - packaging		10 cm	30 cm	straight	14 cm + straight
EO efficiency		41%	30%	30%	39%
Reliability			Photodarkening Splice strength	To be tested	
Vendors			NKT Photonics	AdValue Photonics NP Photonics	INO cfs (custom)
Beam-combinable pulse energy			0.2mJ	1mJ	>0.2mJ

CAP-9  
6 March 2018

LINCOLN LABORATORY  
MASSACHUSETTS INSTITUTE OF TECHNOLOGY

Figure 10. Requirements for the small-sat-ladar transmitter.

**This page intentionally left blank.**

## 8. PHOTON-COUNTING RECEIVER

The small-sat ladar will use a photon-counting APD array. MIT LL has pioneered the development of these APD focal planes. Figure 11 shows four different options for the small-sat ladar. The 32 x 32 asynchronous readout APD array has been successfully used in fielded ladar system; its format is, however, too small for the small-sat ladar. The 256 x 64 APD array has also been successfully use in a fielded ladar system; its readout rate, however, is too low for the small-sat ladar. The focal plane chosen for the small-sat ladar is a 256 x 256 array with asynchronous readout. This APD requires modest, straightforward development compared to existing APDs. We note that existing APD arrays have been radiation tested and no radiation problems are anticipated for the new APD array, particularly given the benign radiation environment at 220 km.



### IR Geiger-Mode APD Options for Small-Sat Ladar

	32x32 Async	256x64 Sync	256x128 Sync	256x256 Async
<b>Format</b>	32x32	256x64	256x128	256x256
<b>Time Resolution (ns)</b>	0.75	1	1	~ 1
<b>Frame Rate (kHz)</b>	1,250	20	100	>1,000
<b>PDE</b>	35%	30%	30%	35-60%
<b>Pixel Pitch (μm)</b>	100	50	50	25
<b>Power (W)</b>	1.3	1.4	3.5	TBD
<b>Alternate modes</b>	Passive, coherent	Minimal passive	Minimal passive	Passive, coherent
<b>Detector Status</b>	Fielded	Fielded	EDU grade	Early development

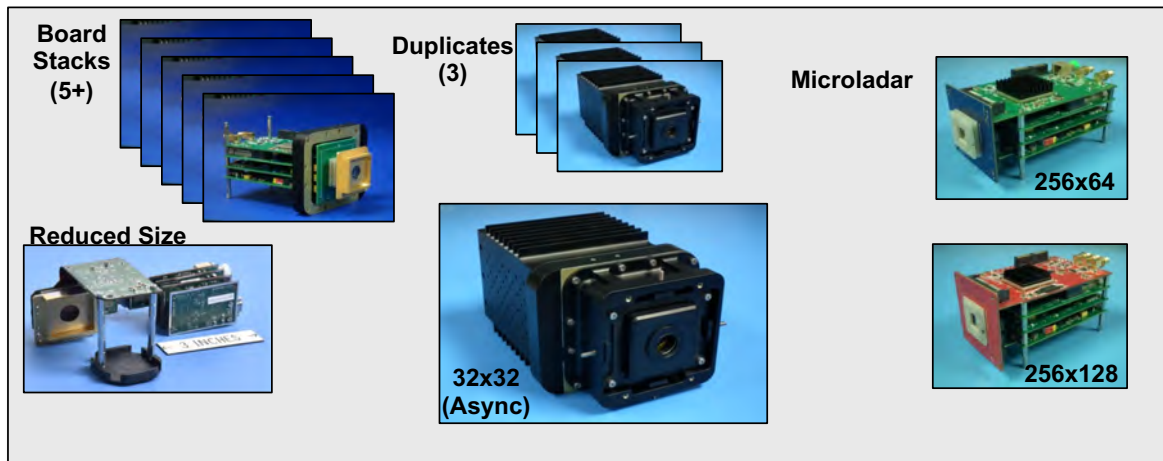
- Synchronous 256x128 detector best choice among mature designs
- Future 256x256 detector best choice after development

Figure 11. Four different focal-plane options for the small-sat ladar.

An APD array by itself does not constitute a receiver; it must be built into a camera. Figure 12 illustrates various modular Geiger-mode APD cameras that have been designed and built at MIT LL over the last few years. With few modifications, the modular camera should be suitable for the small-sat ladar.



## Modular Geiger-Mode APD Cameras Designed and Built 2015-2017



- Async camera design includes Mil-flow parts, is flight (aircraft) qualifiable and thermally tested design
- With little or no modification the modular camera should be suitable for the small-sat ladar

Figure 12. Modular Geiger-mode APD cameras.



## 9. DATA-DRIVEN REGISTRATION

A technical challenge for any 3D-ladar mapping system is registering the individual image chips in the presence of blurring from angular pointing jitter. This challenge has been successfully met in airborne ladar systems, such as ALIRT and MACHETE, but these systems had a relatively easier jitter problem because the ground sample distance (GSD) was larger than the ground resolution distance (GRD) and because there was only a few-kilometer lever arm for the jitter. In addition, these airborne systems could use precise, but large-SWaP pointing mirrors to provide precise pointing knowledge. The small-sat ladar has a more difficult jitter problem. The GSD is  $\lesssim$  GRD, and there are 100s of kilometers of lever arm for the jitter. In addition, for the small-sat ladar it is desirable to eliminate large, expensive precise pointing mirrors.

For the small-sat ladar, we investigated image-based registration using either co-boresighted passive imagery or the ladar data. We found that using the ladar data gave better performance and also allowed night or day operation. Key features of the data-driven jitter compensation are given in Figure 13.



### Data-Driven Jitter Compensation

- **Concurrently solves for both the pulse-by-pulse angle jitter and the pixel-by-pixel true height of the scene**
  - Also evaluates whether a given received photo-electron is signal or noise
- **Optimized for the low per-pulse signal rate of the satellite ladar ( $<0.005$  PE/pixel/pulse) and high repetition rate ( $>200$  kHz)**
- **Uses the  $\sim 16,000$  scene pixels to estimate angular jitter ( $< 100$  PE's/pulse spread over the array)**
- **Uses  $\sim 2,500$  sequential pulses to estimate scene height at each pixel every  $\sim 12.5$  ms**

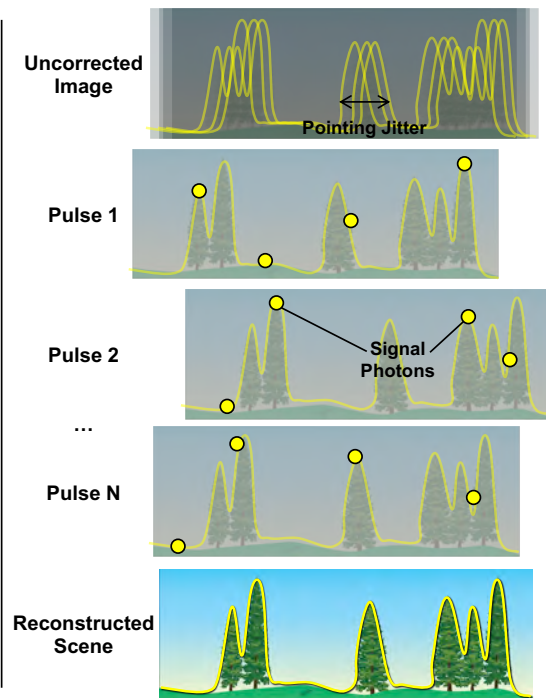


Figure 13. Data-driven jitter compensation.

A simulation of the data-driven jitter compensation is shown in Figure 14. The simulation started with high-quality 3D-ladar data taken over Boston Common using the airborne MACHETE ladar system. The upper-left image is an angle-angle-range image taken by MACHETE; it has GSD of 25 cm, 30 detections per pixel, and < 10-cm rms jitter. The upper-right image is the same image degraded to simulate a small-sat ladar raw image; it has a GSD of 57 cm, only 10 detections per pixel, and 2.2 m rms jitter (i.e., a jitter of about four times the size of a pixel). This simulated raw image is clearly much worse than the original MACHETE image. When the jitter compensation is invoked, the image is much improved, as shown in the lower right. The jitter has been reduced to < 20 cm rms (corresponding to about 1/3 pixel), and the height map correspond well to the original MACHETE image.

The data-driven jitter compensation has been proven to work over a large range of simulated conditions. Further information on the jitter compensation may be found in these documents.<sup>vii,viii</sup>

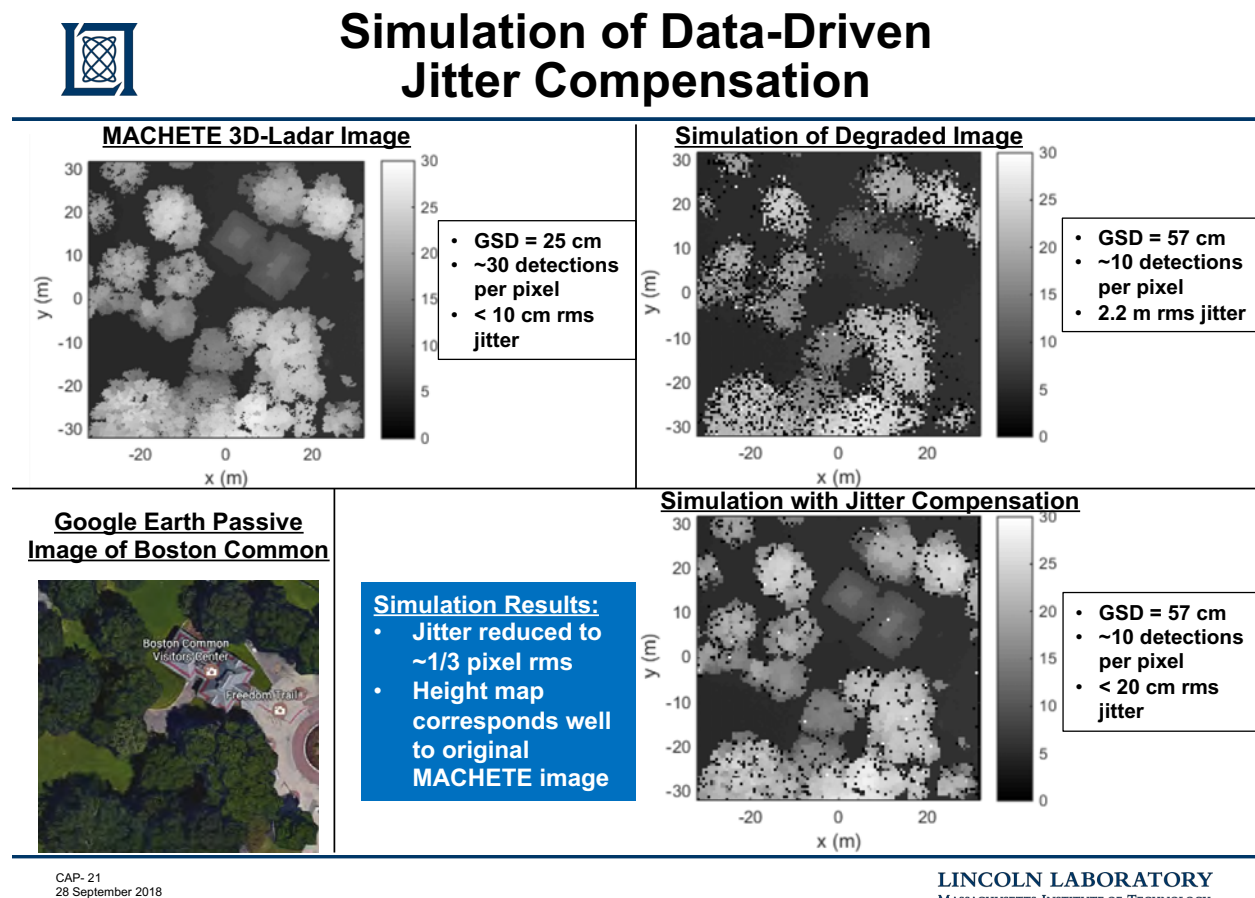


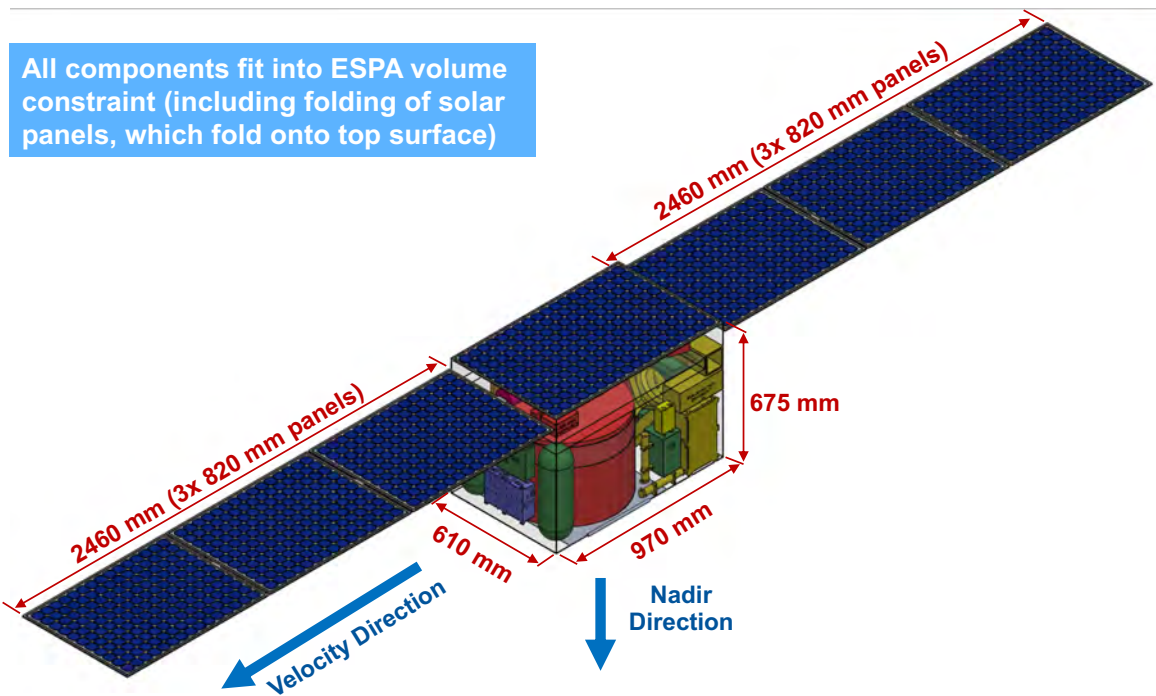
Figure 14. Simulation of the data-driven jitter compensation.

## 10. PACKAGING

As shown in Figure 15, all components of the small-sat ladar fit into a 61-cm x 67.5-cm x 97-cm ESPA volume. Before unfolding the seven 82-cm long solar panels also fit in the ESPA volume.



### Small-Sat-Ladar Packaging



CAP-22  
25 July 2018

LINCOLN LABORATORY  
MASSACHUSETTS INSTITUTE OF TECHNOLOGY

Figure 15. Small-sat-ladar packaging.

Figure 16 shows front and back isometric views of the small-sat-ladar system, with the solar panels removed for clarity. The 50-cm receive telescope takes the most space, followed by the propulsion system. The transmitter and receiver optics are folded around to fit in the constrained volume available.

Further information on the packaging may be found in this document.<sup>ix</sup>



## All Small-Sat-Ladar Subsystems (Solar Panels not Shown)

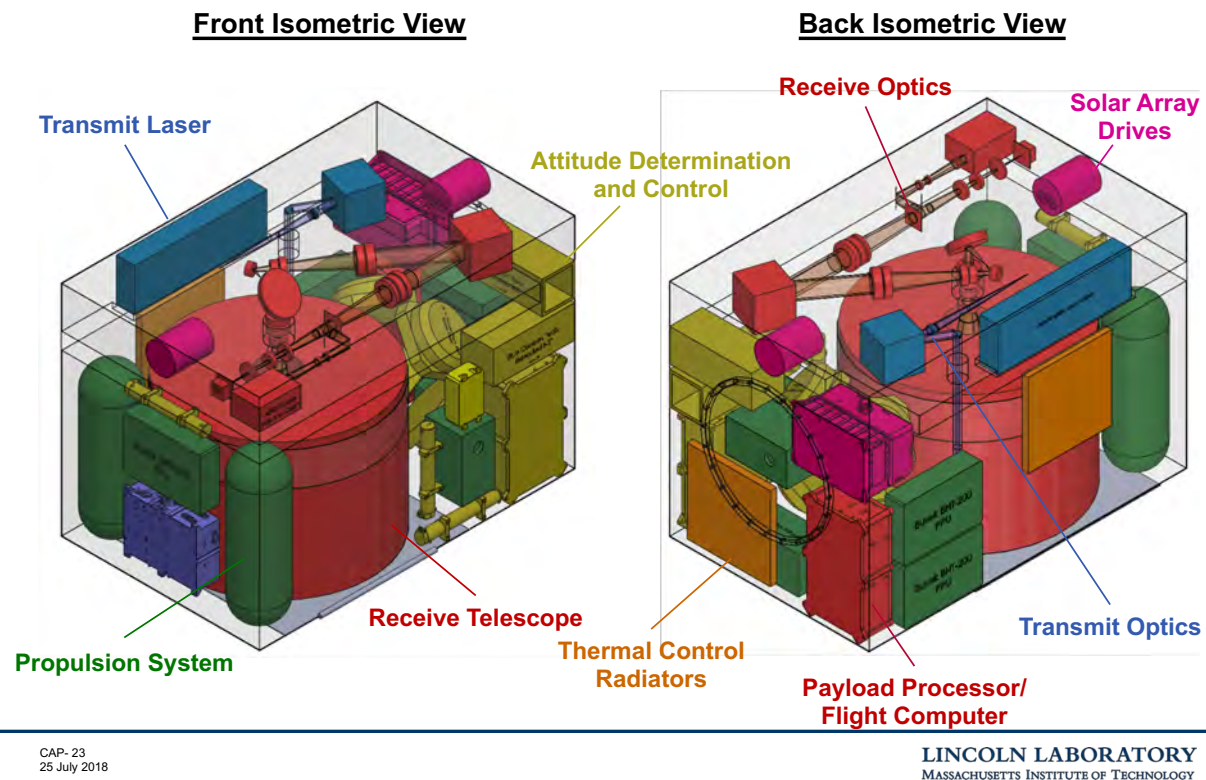


Figure 16. Front and back isometric views of the small-sat-ladar system.

Figure 17 shows estimates of the mass and power allocations. The estimated wet mass is 170 kg—well within the 220 kg limit currently qualified for an ESPA-class system. The mass is reasonably well distributed among the various components, with the receiver, the fuel for electric propulsion, and the support structure being the three most massive elements.

The estimate for orbit-average power is 230 W. This value is high but doable for an ESPA-class system. The orbit-average power is dominated by the electric propulsion, which must be on continuously to maintain the 220-km orbit. Interestingly, the laser transmitter, which is often the driver for power in other systems, accounts for a fairly small fraction of the orbit-average power for the small-sat ladar. Given that, it is likely that the duty cycle could be increased over the currently assumed 2%, with only modest changes in the overall system.



## SWaP Allocation

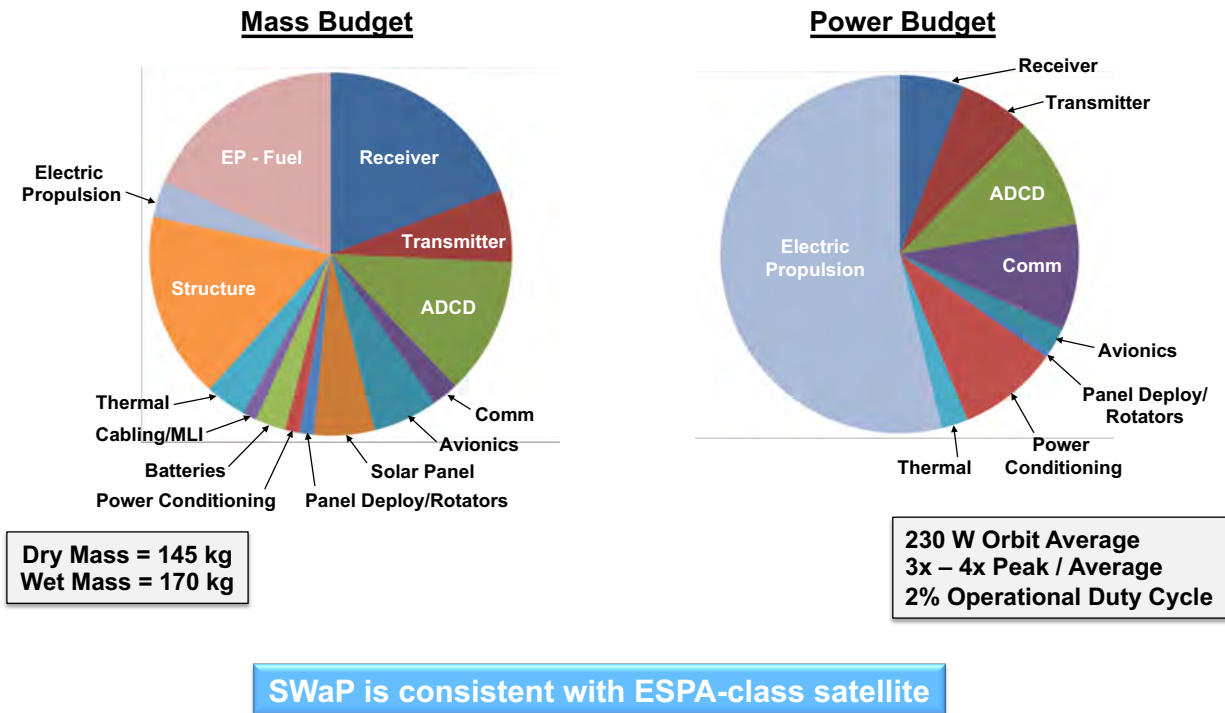


Figure 17. Estimates of the mass and power allocations.

**This page intentionally left blank.**

## 11. CONCLUSIONS

We developed a design concept for a small-sat lidar. The concept developed has the following general characteristics:

- it uses efficient fiber lasers and photon-counting detectors to achieve high performance in a low-weight system;
- it fits in an ESPA-class satellite;
- it flies in a very low orbit ( $\sim 220$  km) to get  $\sim 50$ -cm cross-range resolution at nadir; and
- it is able to generate image areas of about  $10 \text{ km}^2$ .

Based on our design analysis, we conclude that it should be possible to field a high-performance space-based lidar in a relatively low-cost small-sat package.

**This page intentionally left blank.**



## REFERENCES

- i Robert Knowlton, “Airborne Ladar Imaging Research Testbed, MIT Lincoln Laboratory Tech Notes (2011). Available on line at <https://apps.dtic.mil/dtic/tr/fulltext/u2/a594035.pdf>.
- ii Brian F. Aull, Erik K. Duerr, Jonathan P. Frechette, K. Alexander McIntosh, Daniel R. Schuette, and Richard D. Younger, “Large Format Geiger-Mode Avalanche Photodiode Arrays and Readout Circuits, IEEE Journal of Selected Topics in Quantum Electronics, vol 24, no. 2 (March/April 2018).
- iii National Research Council, *Laser Radar—Progress and Opportunities in Active Electro-Optical Sensing*, The National Academies Press (2104).
- iv PE 0602234D8Z
- v Philip D. Chapnik, “Space-Based Ladar Optical Design,” MIT Lincoln Laboratory Project Memorandum 09-PM-SSL-5 (to be published).
- vi John K. Kim, “Development of a space-qualified transmitter for a small-sat 3D ladar,” MIT Lincoln Laboratory Project Memorandum 09-PM-SSL-8 (to be published).
- vii E. J. Phelps and C. A. Primmerman, “Blind Compensation of Angular Jitter for Satellite-Based Ground-Imaging Ladar: FY17 Line-Supported Integrated Systems Project,” MIT Lincoln Laboratory Project Report LSP-221 (22 December 2017).
- viii E. J. Phelps, “Data-Driven Jitter Compensation Parameter Sweep Results,” MIT Lincoln Laboratory Project Memorandum 09-PM-SSL-4 (to be published).
- ix Mark J. Silver, “Small-Sat-Ladar Packaging,” MIT Lincoln Laboratory Project Memorandum 09-PM-SSL-7 (to be published).